Safe Autonomous Flare and Landing during Autorotation through Wind Shear

Nicholas Grande
nag5040@psu.edu
Graduate Research Assistant

Jack W. Langelaan
jlangelaan@psu.edu
Associate Professor

Department of Aerospace Engineering
The Pennsylvania State University
University Park, PA

ABSTRACT

This paper presents a method to compute the set of steady state autorotation conditions from which safe flare to landing through can be performed. Equations of motion of a helicopter in autorotation through wind shear are presented; these equations are used to compute an optimal trajectory to landing from candidate initial states (distance and height above the touchdown point, horizontal speed, descent rate, rotor speed) to a designated touchdown point. The effect of wind shear on these optimal trajectories and on the set of safe initial conditions is examined for two rotorcraft: the Bell OH-58A and a small electric-powered helicopter. The feasibility of using waypoint following control for autorotation landing is examined for the electric-powered helicopter.

NOTATION

C	Cost Function
c_{d0}	Main Rotor Profile Drag Coefficient
C_P	Power Coefficient
C_T	Thrust Coefficient
C_x	Horizontal Component of Thrust Coefficient
C_z	Vertical Component of Thrust Coefficient
d	Horizontal Distance from Touchdown Point
f_e	Fuselage Equivalent Flat Plate Area
f_G	Ground Effect Factor
f_I	Induced Velocity Factor
h	Height above Touchdown Point
H_R	Rotor Height
I_R	Main Rotor Polar Moment of Inertia
m	Mass
R	Main Rotor Radius
u	Horizontal Velocity
u_{20}	Wind Velocity at 20 feet
v_h	Hover Induced Velocity
w	Descent Rate
w_x	Horizontal Wind Velocity
x	horizontal position
z_0	Surface Roughness
α	Main Rotor Tip Path Plane Angle
λ	Main Rotor Inflow Ratio
σ	Main Rotor Solidity
ρ	Air Density
Ω	Main Rotor Angular Speed

Presented at the AHS 69th Annual Forum, Phoenix, Arizona, May 21–23, 2013.

INTRODUCTION

The use of autonomous rotorcraft in safety-critical missions such as casualty evacuation or in missions where the payload is critical (such as resupply missions or missions involving complex, expensive sensor packages) leads to the requirement for safe recovery in the event of a vehicle failure. In particular, loss of power to the main rotor is recoverable through autorotation.

However, autorotation continues to be a difficult maneuver, with the flare phase being especially difficult. The combination of high descent rates and limited energy available in the rotor to arrest descent (and reduce forward speed) means that correct timing of the flare maneuver is critical. Practice autorotations remains part of the training curriculum for pilots. While the problem of autorotation is somewhat mitigated in multi-engine aircraft, most autonomous rotorcraft are single engine vehicles.

The use of optimal control to recover manned helicopters under partial or total power loss has been investigated (Refs. 1–3). Additionally, several researchers have investigated trajectory planning for unmanned rotorcraft in the event of engine failure (Refs. 4–6). While these investigations yield promising results, they all assume ideal conditions; namely, no wind and a flat, obstacle-free landing site. Wind (and especially wind shear) can have a significant effect on the safety of autorotation. Further, computing a safe, feasible flare trajectory in real time is extremely difficult: the problem is high-dimensional and only limited computational resources are likely to be available on board the helicopter. Additionally,

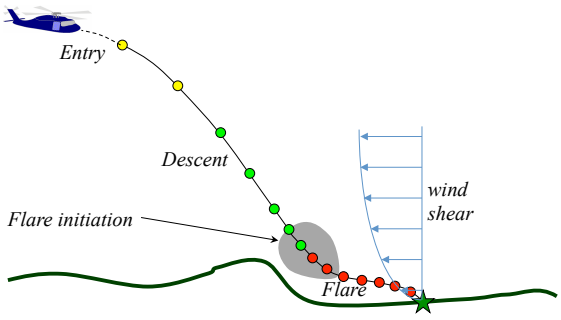

Fig. 1. Schematic of the autorotation scenario.

the existence of a solution is dependent on the initial conditions.

In (Ref. 7), the authors describe the *safe landing set*, namely the set of all points in the helicopter's steady-state autorotation space (defined by horizontal speed, descent rate, and rotor speed) combined with a height above and distance to the desired touchdown point from which a safe path to touchdown is *guaranteed* to exist. This safe landing set is the backwards reachable set from safe touchdown: any vehicle that enters this set is thus guaranteed to have a safe path to ground. The use of backwards reachable sets for safe (powered) landing of fixed wing aircraft is also described in (Refs. 8, 9).

The research presented here extends the safe landing set to account for winds and wind shear. It computes safe landing sets for wind conditions ranging from strong headwinds to light tailwinds for two rotorcraft: the OH-58A and the Adaptive Flight Hornet Mini (a 55" rotor diameter autonomous helicopter). Finally, it uses the Hornet Mini simulation environment to demonstrate (in simulation) safe flare and landing using the Hornet Mini's waypoint tracking controller.

PROBLEM DEFINITION

The problem under consideration is a helicopter initiating and proceeding through the flare phase of autorotation under the influence of wind shear (Figure 1). At flare initiation, the vehicle is transitioned from a steady-state descent to the flare maneuver. The initiation point is characterized by the helicopter's trimmed forward speed (u), descent rate (w), and rotor speed (Ω), as well as a point in space at which the initiation occurs (x, h). The wind velocity at a given altitude is incorporated into the equations of motion, making u and w direct measures of airspeed with respect to the body axes. The resulting state vector can be written as:

$$\mathbf{x} = [\, u \; w \; \Omega \; x \; h \,]^T \tag{1}$$

The control inputs used throughout the trajectory are the main rotor thrust coefficient and tip-path-plane angle.

$$\mathbf{u} = [\, C_T \; \alpha \,]^T \tag{2}$$

These inputs are used to control the airspeeds and rotor speed of the helicopter throughout the maneuver. The flare maneuver ends when the helicopter has reached the ground. The height above touchdown, h, is a relative measure of altitude with respect to the vehicle landing gear. Therefore, landing is known to occur when $h = 0$.

Head wind and tail wind conditions will influence the flight of the helicopter during flare. As the altitude decreases, the magnitude of the wind velocity also decreases, which alters the airspeed of the helicopter. The helicopter is in autorotation, meaning no power can be supplied to the rotor, and there is limited stored energy to slow the vehicle's velocity. Therefore, head winds and tail winds of varying magnitudes will alter the region of the autorotation state space from which a safe path to touchdown exists.

The problem, therefore, is to find the set of initial conditions from which a safe flare path to touchdown through wind shear is guaranteed to exist. This set (denoted the safe landing set) can then be used as the target state for manned autorotation scenarios (i.e. as guidance to the condition at which flare should be initiated) and as the target state for descent phase autorotation path planners (Refs. 10, 11).

Defining the Shear Profile

The shear model chosen for analysis is an altitude-dependent profile defined in MIL-STD-1797A (Ref. 12). This model assumes that the wind velocity within the profile is restricted to the horizontal direction. The magnitude increases logarithmically with altitude, and is modeled as

$$w_x = u_{20} \frac{\ln(\frac{h}{z_0})}{\ln(\frac{20}{z_0})} \tag{3}$$

Here, u_{20} represents the wind velocity at 20 feet above the ground and z_0 represents the surface roughness. Figure 2 shows a shear profile for $u_{20} = 30$ knots and $z_0 = 0.15$. This surface roughness is dictated by (Ref. 12), and is used for approach and landing flight situations.

This shear model is accurate for relatively low altitudes, making it suitable for flare analysis. It can also be added into existing equations of motion in order to model airspeed. Sign convention allows it to easily model both head winds and tail winds of varying magnitude by manipulating the value of u_{20}.

Three different wind severities are described in (Ref. 12): light, moderate, and severe. The u_{20} values that define these severities, as well as the probability of exceeding the particular wind condition, are given in Table 1.

The safe landing sets for the various head wind and tail wind severities were found for two helicopters: the Bell OH-58A and the Adaptive Flight Hornet Mini.

EQUATIONS OF MOTION DURING AUTOROTATION FLARE

Typically flare during autorotation is a longitudinal maneuver (with little to no lateral deviation in flight path). Wind (especially rapidly changing winds) can have a significant effect on vehicle dynamics.

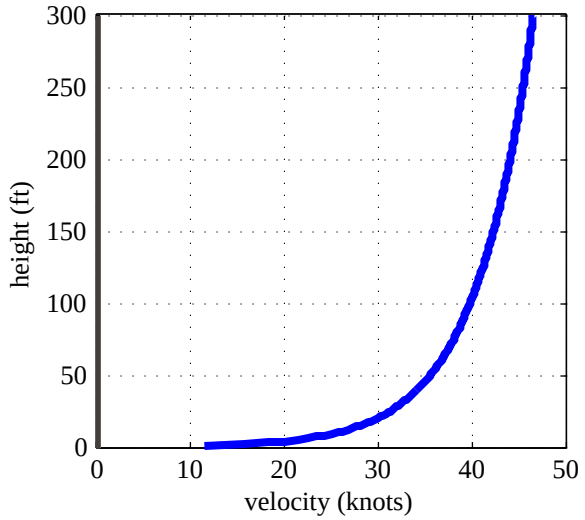

Fig. 2. Wind shear profile.

Table 1. Wind Shear Profile Intensity

Wind Condition	Velocity at 20 ft	Prob. of Exceedance
Light	0 – 10 knots	10%
Moderate	11– 30 knots	0.1%
Severe	31 – 45 knots	0.001%

Autorotation Governing Equations

Equations for a point mass model of a helicopter in autorotation in zero wind are given in Aponso (Ref. 6). These equations can be extended to include the effect of time- or spatially varying wind:

$$m\dot{u} = \rho(\pi R^2)(\Omega R)^2 C_x - \frac{1}{2}\rho f_e u\sqrt{u^2+w^2} + \dot{w}_x \tag{4}$$

$$m\dot{w} = mg - \rho(\pi R^2)(\Omega R)^2 C_z - \frac{1}{2}\rho f_e w\sqrt{u^2+w^2} + \dot{w}_z \tag{5}$$

$$I_R\Omega\dot{\Omega} = P_s - \frac{1}{\eta}\rho(\pi R^2)(\Omega R)^3 C_P \tag{6}$$

$$\dot{x} = u + w_x \tag{7}$$

$$\dot{h} = -(w + w_x) \tag{8}$$

$$\dot{P}_s = \frac{1}{\tau_p}(P_{res} - P_s) \tag{9}$$

Note the overloaded symbols: w denotes helicopter vertical speed (with respect to the air mass) and $\mathbf{w} = [w_x\ w_z]^T$ denotes the wind vector and its components in the horizontal and vertical directions. Further, u denotes helicopter horizontal speed (with respect to the air mass) and u_{20} (which parameterizes the wind shear) denotes wind speed 20 feet above ground level.

Since flare occurs at the end of autorotation it is assumed that the residual power, P_{res}, has decayed away to zero during the descent phase, meaning Equation (9) simplifies to the identity $0 = 0$.

Coefficients are defined as:

$$C_P = \frac{1}{8}\sigma c_{d0} + C_T\lambda \tag{10}$$

$$C_x = C_T \sin\alpha \tag{11}$$

$$C_z = C_T \cos\alpha \tag{12}$$

$$\lambda = \frac{u\sin\alpha - w\cos\alpha + v}{\Omega R} \tag{13}$$

For simplicity, the aircraft pitch angle, θ, is assumed to be approximately equal to the tip-path-plane angle, α. Tip-path-plane angle (an input) is then used in place of pitch in Equation (10) – Equation (13).

The induced velocity is

$$v = K_{ind} v_h f_I f_G \tag{14}$$

where v_h is the hover induced velocity, f_I is the ratio of actual induced velocity to the hover induced velocity, and f_G accounts for the decrease in induced velocity due to ground effect.

$$v_h = (\Omega R)\sqrt{\frac{C_T}{2}} \tag{15}$$

$$f_I = \begin{cases} 1/\sqrt{b^2 + (a + f_I)^2} & \text{if } (2a+3)^2 + b^2 \geq 1 \\ a(0.373a^2 + 0.598b^2 - 1.991) & \text{otherwise} \end{cases} \tag{16}$$

$$f_G = 1 - \frac{R^2\cos^2\theta_w}{16(h + H_R)^2} \tag{17}$$

$$\cos^2\theta_w = \frac{(-wC_T + vC_z)^2}{(-wC_T + vC_z)^2 + (uC_T + vC_x)^2} \tag{18}$$

a and b are

$$a = \frac{u\sin\alpha - w\cos\alpha}{v_h} \tag{19}$$

$$b = \frac{u\cos\alpha + w\sin\alpha}{v_h} \tag{20}$$

It now remains to compute the components of the rate of change of wind speed.

Wind Shear and the Rate of Change of Wind Speed

The total time derivative of wind contains both a time rate of change and the change induced by helicopter motion through a spatial gradient:

$$\frac{d\mathbf{w}}{dt} = \begin{bmatrix} \frac{\partial w_x}{\partial t} \\ \frac{\partial w_z}{\partial t} \end{bmatrix} + \begin{bmatrix} \frac{\partial w_x}{\partial x} & \frac{\partial w_x}{\partial h} \\ \frac{\partial w_z}{\partial x} & \frac{\partial w_z}{\partial h} \end{bmatrix} \begin{bmatrix} u \\ w \end{bmatrix} \tag{21}$$

Recall that the shear model assumes that there is no component of wind in the z direction. Therefore, $\dot{w}_z = 0$ and

$$\dot{w}_x = \frac{\partial w_x}{\partial t} + \begin{bmatrix} \frac{\partial w_x}{\partial x} & \frac{\partial w_x}{\partial h} \end{bmatrix} \begin{bmatrix} u \\ w \end{bmatrix} \tag{22}$$

Additionally, it is assumed that wind speed does not vary with time and there is no gradient in the horizontal direction. Therefore

$$\dot{w}_x = \frac{dw_x}{dh} w \tag{23}$$

Incorporating Equation (3),

$$\dot{w}_x = \frac{u_{20}}{\ln(\frac{20}{z_0})} \frac{w}{h} \tag{24}$$

Equations of motion for a helicopter in autorotation through wind shear can now be summarized:

$$m\dot{u} = \rho(\pi R^2)(\Omega R)^2 C_x - \frac{1}{2}\rho f_e u\sqrt{u^2+w^2} + \frac{u_{20}}{\ln(\frac{20}{z_0})}\frac{w}{h} \tag{25}$$

$$m\dot{w} = mg - \rho(\pi R^2)(\Omega R)^2 C_z - \frac{1}{2}\rho f_e w\sqrt{u^2+w^2} \tag{26}$$

$$I_R \Omega \dot{\Omega} = P_s - \frac{1}{\eta}\rho(\pi R^2)(\Omega R)^3 C_P \tag{27}$$

$$\dot{x} = u + u_{20}\frac{\ln(\frac{h}{z_0})}{\ln(\frac{20}{z_0})} \tag{28}$$

$$\dot{h} = -w \tag{29}$$

During the flare phase of autorotation, descent rate w is typically positive. In a head wind u_{20} is negative (see Equation (28) for this sign convention). Equation (25) shows (and all pilots will explain) that for a helicopter descending through headwind shear, airspeed will decrease more rapidly than it would for descent in zero wind. This can complicate the problem of flare. One realizes that the opposite would occur for descent through tailwind shear, but in that case the problem will be excessive ground speed.

Height Parameterized Equations of Motion

Throughout the flare maneuver, the control inputs $\mathbf{u}(t)$ are used to manipulate the velocity and position of the helicopter in an effort to reach a safe landing. Continuously changing C_T and α also continuously changes the descent rate. Since the time to touchdown is dictated by the initial height and the descent rate, the variability of the descent rate means that the time of touchdown is not known until it is reached. One solution is to discretize the problem in terms of height, making time an additional parameter. This simplifies the problem because touchdown is known to occur when $h = 0$, regardless of initial states or control inputs. The problem can now be discretized into small height steps, with the assumption that the control input is constant over each step.

Tierney presents a methodology for converting to height parameterized equations of motion, based on a forward Euler integration (Ref. 7) (see Figure 3).

Using that approach, height above touchdown becomes the independent variable, and time becomes a dependent variable. The state vector can now be written as:

$$\mathbf{x} = [\, u \; w \; \Omega \; x \; t \,]^T \tag{30}$$

The height discretized equations of motion for autorotation descent of a helicopter through wind shear can now be written as

$$\mathbf{x}_{k+1} = \mathbf{x}_k + \left.\frac{d\mathbf{x}}{dh}\right|_k \Delta h_k \tag{31}$$

where the components of $\left.\frac{d\mathbf{x}}{dh}\right|_k$ are

$$\frac{du}{dh} = -\frac{1}{mw}\left[\rho(\pi R^2)(\Omega R)^2 C_x - \frac{1}{2}\rho f_e u\sqrt{u^2+w^2}\right] - \frac{u_{20}}{\ln(\frac{20}{z_0})}\frac{1}{h} \tag{32}$$

$$\frac{dw}{dh} = -\frac{1}{mw}\left[mg - \rho(\pi R^2)(\Omega R)^2 C_z - \frac{1}{2}\rho f_e w\sqrt{u^2+w^2}\right] \tag{33}$$

$$\frac{d\Omega}{dh} = -\frac{1}{I_R \Omega_w}\left[P_s - \frac{1}{\eta}\rho(\pi R^2)(\Omega R)^3 C_P\right] \tag{34}$$

$$\frac{dx}{dh} = -\frac{u}{w} - \frac{u_{20}}{w}\frac{\ln(\frac{h}{z_0})}{\ln(\frac{20}{z_0})} \tag{35}$$

$$\frac{dt}{dh} = -\frac{1}{w} \tag{36}$$

This approach has two assumptions: first, descent rate is always positive (i.e. the helicopter cannot "swoop" upwards); second, the time interval Δt_k is short enough that the descent rate over that interval is constant.

Equation (32) further shows that for descent through a headwind shear airspeed will drop more quickly as height is lost than it would for descent in zero wind.

COMPUTING THE SAFE LANDING SET

Here, the methodology for computing the safe landing set for a helicopter acting in wind shear is presented. The algorithm used is an extension of the work developed by Tierney. It builds from that work by involving wind in the measurement of vehicle velocity, making it a true airspeed. To investigate the influence of wind on the flare trajectories of various sized helicopters, the problem parameters were adjusted to the specifications of the OH-58 and the Hornet Mini.

The goal of the safe set algorithm is to computer the safe landing set: the set of all points in the helicopter's steady-state autorotation space, combined with flare initiation points, for which a safe, feasible path to touchdown is guaranteed to exist. Individual trajectories within the set are computed by altering the control inputs, $\mathbf{u}(t)$, throughout the maneuver. The path is optimized by minimizing a cost function dependent on the vehicle states and controls at each step:

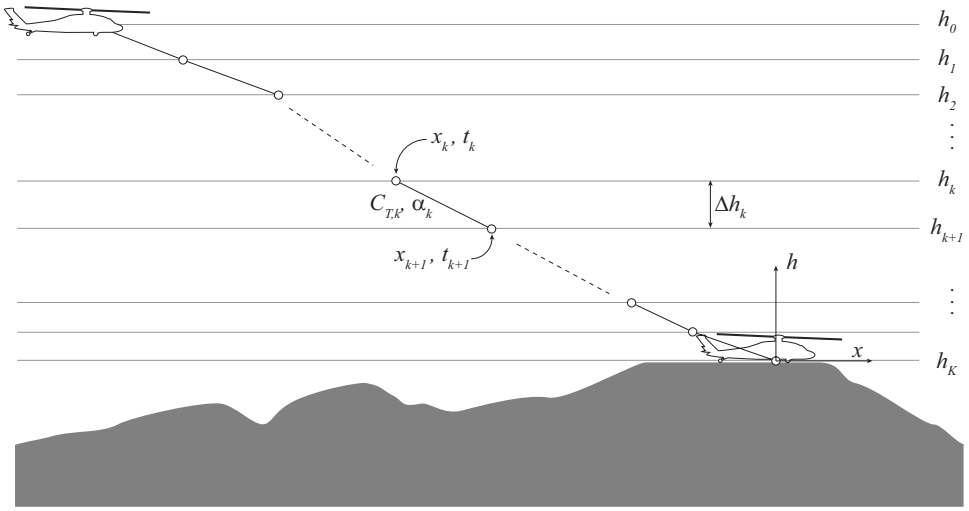

Fig. 3. Schematic of the height-discretized flare trajectory optimization problem. The target touchdown point is at the origin, the shaded region denotes terrain (Ref. 7).

$$\begin{aligned}
&\text{minimize } C(\mathbf{x}_{0\ldots K}, \mathbf{u}_{0\ldots K-1}) \\
&\text{subject to } \mathbf{x}_{k+1} = \mathbf{x}_k + \left.\frac{d\mathbf{x}}{dh}\right|_k \Delta h_k \\
&\qquad \mathbf{x}_{min} \le \mathbf{x}_k \le \mathbf{x}_{max} \\
&\qquad g(\mathbf{x}_k) \le 0 \\
&\qquad \mathbf{u}_{min} \le \mathbf{u}_k \le \mathbf{u}_{max} \\
&\qquad \mathbf{x}_0 = [\, u_0 \; w_0 \; \Omega_0 \; x_0 \; t_0 \,]^T
\end{aligned}$$

The vehicle states at each step are calculated using the states from the previous step and the height-based equations of motion. These states are constrained by operational bounds that are dictated by helicopter-specific performance limitations, as well as wind velocity. The state-dependent constraints, $g(\mathbf{x}_k)$, include considerations such as structural limits. The control limitations are determined by operational restrictions of the vehicle.

The cost function, C, is a weighted sum of the touchdown and state costs:

$$C = C_{td} + \gamma C_{state} \tag{37}$$

where γ is the weight parameter that adjusts the relative weight of the state cost versus the touchdown cost.

State Cost

As the helicopter descends, its states are bounded by operational constraints. These constraints can be represented as a barrier function, illustrated in Figure 4. As the state limitations are approached, the state cost begins to rapidly increase.

The upper and lower constraint limitations are dictated by the autorotative performance capabilities of the helicopter, as well as the wind velocity at the particular altitude. At any point in the flare trajectory, the helicopter must be moving towards the landing site. This means that the ground speed of the vehicle must be positive. The helicopter velocity is measured as airspeed, so the lower limit of the velocity state is determined by the wind speed at that given altitude. Since the shear model is altitude-dependent, the lower limit on airspeed is also altitude-dependent.

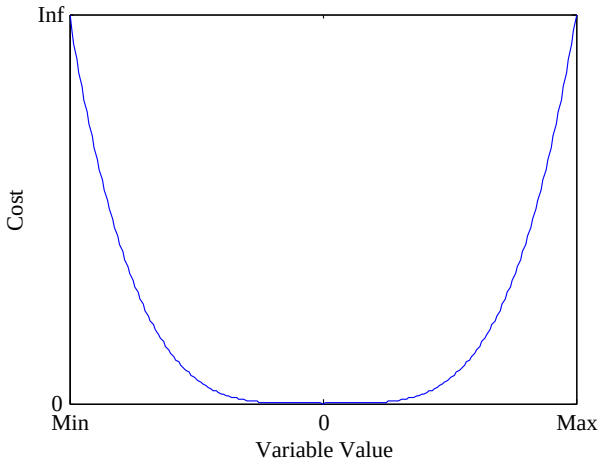

Fig. 4. Sample Barrier Function.

The state cost is calculated at each height step along the path. At the end of the trajectory, these individual state costs are added up to give the total state cost:

$$C_{state} = \sum_{k=1}^{K} c(\mathbf{x}_k) \tag{38}$$

Touchdown Cost

The touchdown cost is determined by the helicopter states when $h = 0$. The designated landing site is defined as a bounded region on either side of the origin. The touchdown cost is dependent only on the helicopter's proximity to the landing site, forward speed and descent rate at touchdown, and the helicopter's pitch angle at touchdown. The touchdown cost is defined as:

$$C_{td} = (\mathbf{x}_K - \mathbf{x}_{des})^T \mathbf{W}_{td} (\mathbf{x}_K - \mathbf{x}_{des}) \tag{39}$$

where $\mathbf{x}_{des}$ are the desired states at touchdown, and $\mathbf{W}_{td}$ is the touchdown weight matrix.

$$\mathbf{W}_{td} = \text{diag}(W_u,\ W_w,\ 0,\ W_d,\ 0,\ 0,\ W_\alpha) \tag{40}$$

Touchdown is assumed to occur when $h = 0$, representing the landing gear touching down. However, the vehicle airspeed is measured from the center of gravity, meaning a component of wind is still acting on the helicopter at touchdown. This means that the landing condition of u is dependent on wind velocity in order to achieve a ground speed within a safe range for touchdown.

Optimization

For a specific wind condition, individual trajectories of the landing set are calculated by iteratively solving the optimization problem for a particular initial condition. MATLAB's *fmincon* function is used to minimize the cost function based on state and control constraints. The generated path is a local minimum which satisfies the requirements of a "safe" solution. The initial guess of control inputs is important in order to avoid getting trapped in a poor local minima that does not yield a safe solution.

The control inputs are represented by a five-point spline. As an initial guess, the thrust coefficient is brought from its trimmed condition to its maximum value at touchdown in an effort to reduce descent rate. The tip-path-plane angle is brought from it's trimmed condition to a high negative value and then back down to the terrain level. This allows the helicopter to "sprint" to the landing site before deccelerating during landing.

The optimization problem can now be written more specifically as:

$$\begin{aligned}
&\text{minimize } C_{td} + \gamma C_{state} \\
&\text{subject to } \mathbf{x}_{k+1} = \mathbf{x}_k + \left.\frac{d\mathbf{x}}{dh}\right|_k \Delta h_k \\
&\qquad \mathbf{x}_{min} \le \mathbf{x}_k \le \mathbf{x}_{max} \\
&\qquad g(\mathbf{x}_k) \le 0 \\
&\qquad \mathbf{u}_{min} \le \mathbf{x}_k \le \mathbf{u}_{max} \\
&\qquad \mathbf{u}_k = spline(U) \\
&\qquad \mathbf{x}_0 = [\ u_0\ w_0\ \Omega_0\ x_0\ t_0\ ]^T
\end{aligned}$$

Throughout the optimization process, the value of γ can be adjusted in order to ensure that a path is found which does not violate constraints. This iterative process is repeated until a path that is both feasible and safe (touchdown constraints are not violated) is found.

Safe Set Algorithm

As in (Ref. 7), the safe landing set is found by repeatedly solving the optimization problem for different initial conditions. Candidate initial states are members of a trimmed set of steady-state autorotation conditions. Various members of this set are tested at each initiation point in the flare region of the helicopter. If the initial states result in a safe path to touchdown, then those states (and the corresponding initiation point) are part of the safe landing set.

Safe landing sets were generated for light, moderate, and severe head winds and tail winds. A safe landing set for the zero-wind case was also generated. These various sets were generated for two helicopters: the OH-58A and the Hornet Mini.

The Bell OH-58A is a utility helicopter used in both military and civilian applications. Properties are given in Table 2 and obtained from (Ref. 13). This aircraft is similar in size to the Northrop Grumman Fire-X autonomous helicopter.

Table 2. Parameters of the OH-58A

parameter	symbol	value
blade chord	c	1.33 ft
rotor profile drag coefficient	C_{d0}	0.0087
equivalent flat plate area	f_e	24 ft^2
rotor height	H_R	9.58 ft
main rotor polar moment of inertia	I_R	1344 slug-ft^2
induced power factor	K_{ind}	1.13
number of blades	N_b	2
rotor radius	R	17.63 ft
gross weight	W	3000 lbs
power efficiency factor	η	0.97

The Hornet Mini UAV (designed by Adaptive Flight) is a small autonomous helicopter based on a commercially available electrically powered radio-controlled helicopter. Parameters are given in Table 3.

The on-board autopilot is capable of several flight modes including GPS waypoint control and kinematic trajectory following control (this mode assumes that the trajectory is dynamically feasible).

RESULTS

To investigate the effect of wind shear on the flare trajectories and safe landing sets of the two aircraft, safe landing sets were computed for winds ranging from strong head wind through

Table 3. Parameters of the Hornet Mini

parameter	symbol	value
blade chord	c	0.177 ft
rotor profile drag coefficient	C_{d0}	0.01
equivalent flat plate area	f_e	0.401 ft^2
rotor height	H_R	1.38 ft
main rotor polar moment of inertia	I_R	0.02 slug-ft^2
induced power factor	K_{ind}	1.15
number of blades	N_b	2
rotor radius	R	2.29 ft
gross weight	W	11.6 lbs
power efficiency factor	η	0.9

zero wind to strong tailwind. In all cases the upper limit of the wind range was used (e.g. 10 knots for light wind, 30 knots for moderate wind and 45 knots for strong wind). The intersection of the safe landing sets for each of these wind conditions (if one exists) indicates the "safest" flare initiation condition.

The high dimensionality of the problem makes the safe landing set difficult to visualize: it is a five dimensional space. One way to effectively visualize the safe set is by utilizing parallel coordinates, as shown in Figure 5 (this is the safe landing set for the OH-58 acting in zero wind).

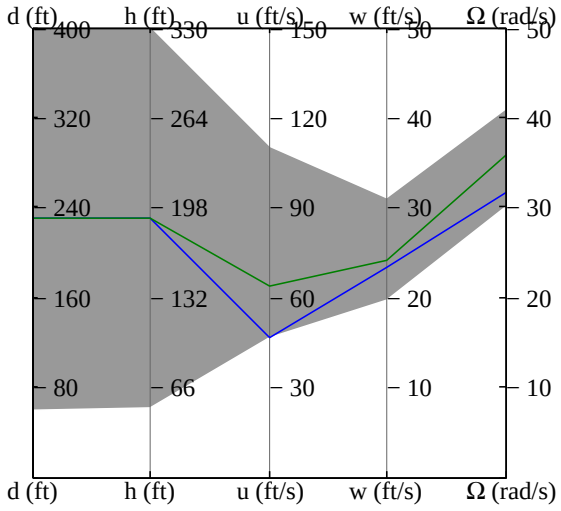

Fig. 5. The bounded region of the safe landing set for the OH-58 in zero wind showing two successful initial states.

Along the x-axis, the two position values (d, h), as well as each of the three states (u_0, w_0, Ω_0), occupy their own coordinate. The various state and position values that result in safe landings are scaled accordingly by the corresponding maximum tested value of each state. The grey area of Figure 5 is the bounded region of the safe landing set.

The two lines within the grey bounded region represent the state combinations of the two safe landings that occurred at the initiation point where $d = -230$ feet and $h = 190$ feet. As can be seen Figure 5, the d and h combinations are the same for the two conditions, since they both occurred at the same flare initiation point. The states values then branch off, each occupying a different location within the bounded region.

OH-58 Safe Landing Sets

To find the safe landing sets for the OH-58, a subset of evenly spaced trimmed initial states was chosen from the set of all trimmed autorotation conditions, and tested at various initiation points in the flare region of the helicopter. The flare region is the bounded distance from and height above the desired landing site from which the helicopter can realistically flare and land safely. For the OH-58, the horizontal distance ranges from 60 feet to 400 feet from the landing site in increments of 10 feet. The height above the landing site ranges from 50 feet to 330 feet in increments of 10 feet. All combinations of trim states and initiation points are tested. If a specific combination results in a feasible path to touchdown, then it is a member of the safe landing set.

As previously mentioned, the aircraft states and controls are bounded by operational limits throughout the maneuver. These constraints can be seen in Table 4. Touchdown limits are given in Table 5.

Table 4. OH-58 State and Control Limits

state/control	symbol	upper	lower
forward airspeed speed	u	169 ft/s	u_w (ft/s)
descent rate	w	40 ft/s	0 ft/s
rotor speed	Ω	390 RPM	248 RPM
thrust coefficient	C_T	$1.5C_w$	0
tip-path-plane angle	α	30°	-30°

Table 5. OH-58 Touchdown Conditions

state	upper	lower
horizontal position	+25 ft	-25 ft
time	–	–
forward ground speed	+ 6 ft/s	0 ft/s
forward airspeed	6 + u_w (ft/s)	0 + u_w (ft/s)
descent rate	+8 ft/s	0 ft/s
rotor speed	–	–
aircraft pitch angle	$\theta_{terrain} + 3.65°$	$\theta_{terrain} - 10°$

Touchdown occurs when the skids reach the ground. Dynamics (and the effect of wind) are computed at the center of gravity, which is approximately 5 feet above the skids. Wind will thus still have a significant effect on the helicopter even at touchdown.

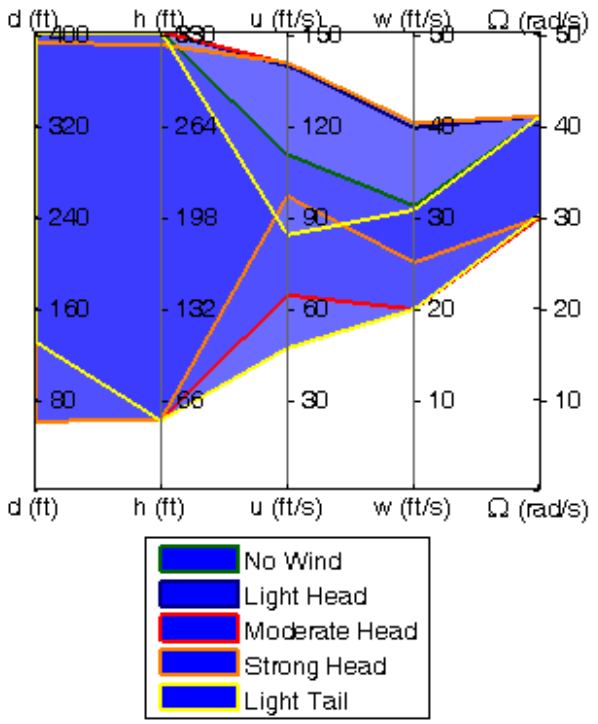

Fig. 6. Total safe landing set for the OH-58 acting in various wind conditions.

Figure 6 shows the five safe landing sets that were found for the various wind conditions. Note the lack of a safe landing set for moderate and strong tailwinds: this indicates that safe autorotation flare cannot be achieved with greater than light tailwinds. With moderate to strong tailwinds the high resulting ground speed leads to either an overshot desired touchdown point or ground speed above limits at touchdown.

This figure also shows that there is no common safe region among the remaining five wind conditions. Two approaches are possible: never land with a tailwind (even a light tailwind), which will leave an intersecting safe landing set for zero wind to strong headwinds; or do not attempt to autorotate into a strong headwind, which will leave an intersecting safe landing set for light tailwinds to moderate headwinds. Analyzing the probabilities of occurrence of the possible desired landing conditions would provide guidance on the correct approach.

Head winds of increasing magnitude shift the forward airspeed range towards its maximum value, and shifts the initiation point closer to the landing site. This is due to the requirement that the helicopter must always be moving towards the landing site. The wind velocity dictated by the shear model increases with altitude. This velocity places a lower limit on airspeeds which do not violate restrictions. If the wind speed is greater than the airspeed at a given altitude, the helicopter must be moving backwards. This condition would always violate the constraints of the algorithm, causing it to fail. At lower initial altitudes, the wind velocity is also lower, broadening the range of allowable airspeeds.

Flaring through a light head wind generated the widest range of initial states that resulted in a safe landing. This is because the head wind increases the allowable airspeed range at touchdown without being so large that it greatly reduces the state constraints throughout the trajectory. This indicates that for the OH-58, a light head wind (even with wind shear) is beneficial when trying to flare during autorotation.

In order to demonstrate the influence of wind on individual trajectories within the Safe Landing Set, three trajectories were analyzed: one under the influence of a light head wind, one under the influence of a light tail wind, and one flying in zero wind conditions. In each case, the flare maneuver was initiated from the same initiation states and position. Flare was initiated a position 340 feet away from, and 240 feet above, the designated touchdown point. The helicopter was flying with a forward speed of 49.4 ft/s, a descent rate of 24.2 ft/s, and a rotor speed of 324 RPM, which is 91.5% of the nominal rotor speed. The three trajectories can be seen in Figure 7(a) and the state comparisons can be seen in Figure 7(b).

Hornet Mini Landing Sets

A similar process was used to find the safe landing sets for the Hornet Mini UAV. The Hornet is considerably smaller and slower than the OH-58, resulting in a correspondingly smaller flare region. The horizontal distance of the region ranges from 15 feet to 50 feet from the landing site in 5 foot increments. The height above the landing site ranges from 10 feet to 30 feet, also in 5 foot increments. The trim states that result in a safe landing are a part of the safe landing set. One consequence of the small size of the Hornet Mini is the very high wind shear it experiences at touchdown: the logarithmic wind model of Equation (3) has very high gradient close to the ground. This high shear complicates the final moments of touchdown.

Vehicle state and control constraints are given in Table 6. Touchdown limits are given in Table 7.

Table 6. Hornet State and Control Limits

state/control	symbol	upper	lower
forward airspeed speed	u	50 ft/s	u_w (ft/s)
descent rate	w	20 ft/s	0 ft/s
rotor speed	Ω	1947 RPM	1416 RPM
thrust coefficient	C_T	$1.5C_w$	0
tip-path-plane angle	α	30°	-30°

Severe winds (above 31 knots) are higher than the Hornet Mini's maximum airspeed. Since safe flight cannot occur in greater than moderate winds, safe autorotation cannot occur in greater than moderate winds.

Safe landing sets are shown in Figure 8. There were no conditions where safe flare could occur in tailwinds, and the moderate headwind results in a very narrow safe landing set (shown by the bounded red region). With tailwinds the Hornet

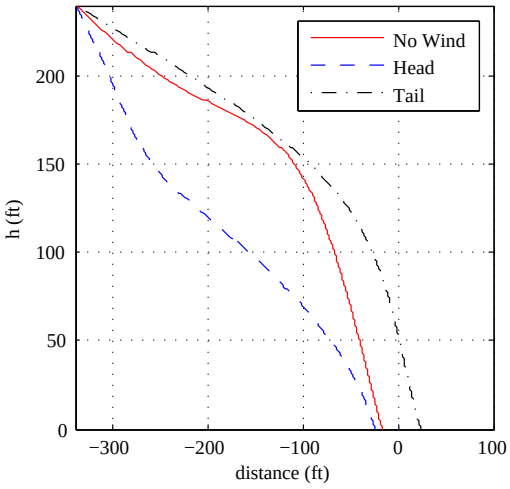

(a) flight path

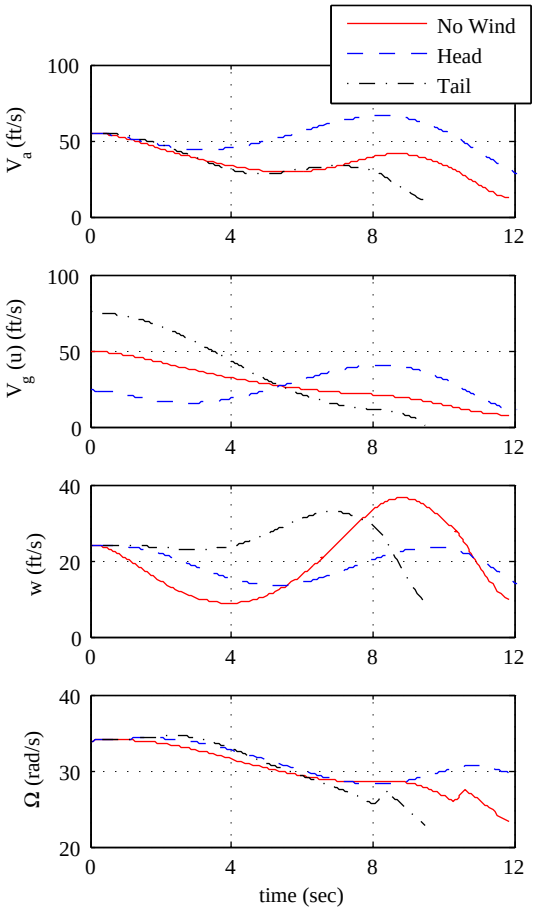

(b) state history

Fig. 7. Flare trajectories for the OH-58 starting at the same initial conditions under light head wind, light tail wind, and no wind conditions.

Table 7. Hornet Touchdown Conditions

state	upper	lower
horizontal position	+10 ft	-10 ft
time	–	–
forward ground speed	+ 5 ft/s	0 ft/s
forward airspeed	$5 + u_w$ (ft/s)	$0 + u_w$ (ft/s)
descent rate	+6 ft/s	0 ft/s
rotor speed	–	–
aircraft pitch angle	$\theta_{terrain} + 5°$	$\theta_{terrain} - 5°$

Mini is unable to reduce its ground speed to the safe bounds during flare.

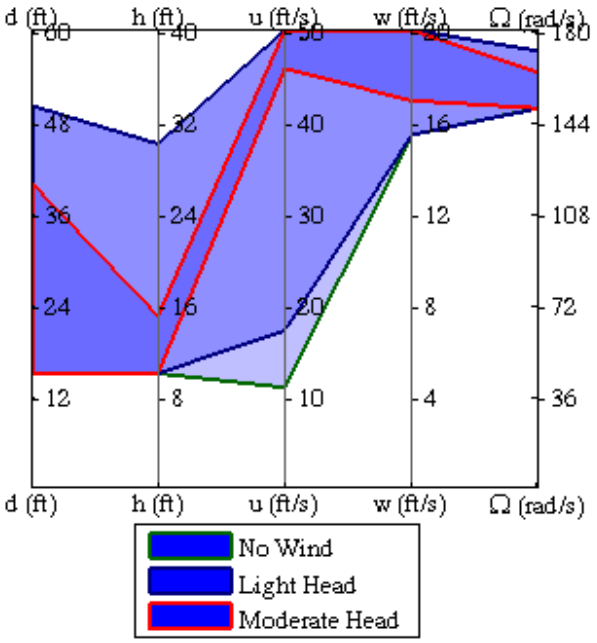

Fig. 8. Total safe landing set for the Hornet in various wind conditions.

As can be seen in Figure 8, the ideal flare initial states live near their respective maximum values. Conversely, the initiation points are close, both vertically and horizontally, to the landing site. High wind conditions greatly constrict the flare region which result in safe landings. When operating in a moderate wind condition, the Hornet must fly fast and flare late. As opposed to the OH-58, calmer conditions are ideal in order to maximize the flare success rate of the Hornet.

A flare trajectory was generated for the same set of initial states under light head wind and no wind conditions. Initiation occurred 50 feet away from and 20 feet above the desired touchdown point. The path was generated using an initial forward speed of 38.5 ft/s, descent rate of 19.5 ft/s, and rotor speed of 1600 RPM, which is 90.4% of the nominal rotor speed for this helicopter. The trajectories can be seen in Figure 9(a) and the state comparisons can be seen in Figure 9(b).

Table 8. Hornet Mini planned and simulated touchdown conditions (using GPS waypoint navigation).

state	planned	simulated
u	4.3 ft/s	3.1 ft/s
w	5.5 ft/s	3.1 ft/s

Hornet Simulation

The Hornet Mini simulation environment was used for testing autonomous flare. The Hornet Mini is capable of trajectory following control, but in the preliminary tests reported here GPS waypoint following is used for flare.

In the Hornet Mini's controller, a waypoint includes GPS position and altitude as well as a commanded airspeed and descent rate. One can thus place a waypoint in the safe landing set for a desired touchdown location and place a zero velocity waypoint (a "stop at" waypoint) at the desired touchdown location. The onboard controller generates a trajectory between these waypoints that meets the desired endpoint criteria (Ref. 11). In practice the touchdown waypoint was placed a small distance above ground (about three feet) to account for overshoot. The vehicle will attempt to come to a stop at the touchdown waypoint and will attempt to maintain hover. With no power going to the rotor it will then settle to touchdown.

To test autorotation flare using waypoint control, a third waypoint (a simulation initial condition) is required. This initial condition waypoint is defined with airspeed and descent rate at the desired flare initiation condition and at a location above and behind the flare initiation point (so that the flight path is consistent with airspeed and descent rate: see Figure 10 for a screen shot).

A flare initiation point near the middle of the Hornet's zero-wind safe landing set (Figure 8) was defined as a waypoint: $x = 30$ feet, $h = 20$ feet, $u = 23.1$ ft/s, $w = 18.6$ ft/s, and $\Omega = 1562$ RPM. Placing the touchdown waypoint at an altitude of three feet resulted in safe landing, with planned and actual touchdown conditions given in Table 8. Note that touchdown at a vertical speed of 3 ft/s is equivalent (in terms of energy) to the helicopter being dropped to the ground from a height of 2 inches.

A comparison of planned and simulated trajectories is shown in Figure 11. Flight paths are very similar. Note that the waypoint following controller results in touchdown at the desired point: the trajectory obtained from the safe set merely seeks touchdown within 10 feet of the desired location. Forward speed, descent rate, and rotor speed vary more smoothly in the GPS-waypoint simulated trajectory. This is partially due to the higher order dynamics in the simulator (recall that the trajectory generator used in the safe set computation is a point mass model).

Control inputs (longitudinal cyclic and collective) are plotted as fraction of maximum possible. Both are well within bounds, indicating that the flare trajectory is not "over taxing" the vehicle's control authority.

A remaining question is the sensitivity of safe touchdown to the height of the touchdown waypoint above ground and the position of the flare initiation waypoint. The flare initiation waypoint height was varied ± 2 feet around the nominal value of 20 feet with minimal effect on touchdown; the touchdown waypoint height was varied from 1 foot above ground to 5 feet above ground and safe (within bounds) touchdown was still observed. This gives confidence in the use of GPS waypoint control for flare trajectories, and means that the ultimate purpose of the safe set algorithm (which was to generate the set of safe flare initial conditions) is broadly applicable to rotorcraft autorotation.

CONCLUSIONS

This paper has extended earlier work defining the safe landing set (the set of all steady state autorotation conditions combined with an altitude above and a distance to a desired touchdown point) to include autorotation through wind shear.

Winds affect both the autorotation state and the position from which flare should be initiated. Computing the safe landing set for the Bell OH-58A confirmed that autorotation landing should not be done with tailwinds above light strength and showed that there is a region in the autorotation state space that permits flare to landing in headwinds ranging from calm to strong. This condition (in the intersection of the safe landing sets for the various wind conditions) should therefore be used as the target flight condition for flare initiation. Light headwinds resulted in the largest safe landing set for the OH-58A.

Computing the safe landing set for a small electrically powered helicopter (Adaptive Flight Hornet Mini) showed that safe flare is not possible in strong winds (which are in any case greater than the maximum airspeed of that vehicle). For the Hornet Mini the largest safe landing set occurs in zero wind: this is not surprising, since small, lightweight, slow vehicles are more strongly affected by wind than larger vehicles.

The Hornet Mini's simulation environment was used to test the feasibility of using GPS waypoint control for flare. Three waypoints defined flare: a touchdown that should be placed approximately 3 feet above ground; a flare initiation waypoint that is in the safe landing set; and a flight path waypoint to help place the vehicle in the correct flight condition as the safe set is entered. Safe touchdown occurred even with significant variation in waypoint altitudes, indicating that GPS waypoint control is a feasible means of performing flare (at least for small helicopters).

ACKNOWLEDGMENTS

This project was funded by the Vertical Lift Consortium under Project Number B-31-02.1-A05. The authors would like to thank Dr. Joseph Horn and Thanan Yomchinda for their collaboration and insight throughout the project. The authors would also like to extend a special thanks to Dr. Eric Johnson of Adaptive Flight for his ongoing technical assistance during the implementation of the Hornet Mini UAS.

REFERENCES

[1]Johnson, W., "Helicopter Optimal Descent and Landing after Power Loss," Technical Memorandum TM 73244, May 1977.

[2]Leishman, J. G., *Principles of Helicopter Aerodynamics*, Cambridge University Press, New York, NY, 2006, Chapter 5.

[3]Floros, M. W., "DESCENT Analysis for Rotorcraft Survivability with Power Loss," American Helicopter Society 65th Annual Forum, Grapevine, TX, USA, 2009.

[4]Bachelder, E. N. and Aponso, B. L., "Using Optimal Control for Helicopter Autorotation Training," Proceedings of the American Helicopter Society 59th Annual Forum, May 6-8 2003.

[5]Abbeel, P., Coates, A., Hunter, T., and Ng, A. Y., "Autonomous Autorotation of an RC Helicopter," International Symposium on Robotics, 2008.

[6]Aponso, B., Lee, D., and Bachelder, E. N., "Evaluation of a Rotorcraft Autorotation Training Display on a Commercial Flight Training Device," Proceedings of the American Helicopter Society 61st Annual Forum, 2005.

[7]Tierney, S. and Langelaan, J. W., "Autorotation Path Planning using Backwards Reachable Sets and Optimal Control," Proceedings of the 66th AHS Annual Forum, May 11-13 2010.

[8]Sprinkle, J., Eklund, J. M., and Sastry, S. S., "Deciding to Land a UAV Safely in Real Time," Americna Controls Conference, Portland, OR, USA, 2005.

[9]Bayen, A. M., Mitchell, I. M., Oishi, M. M. K., and Tomlin, C. J., "Aircraft Autolander Safety analysis Through Optimal Control-Based Reach Set Computation," *Journal of Guidance and Control*, Vol. 30, (1), January-February 2007, pp. 68–77.
doi: 10.2514/1.21562

[10]Holsten, J., Loechelt, S., and Alles, W., "Autonomous Autorotation Flights of a Helicopter UAVs to Known Landing Sites," Proceedings of the 66th AHS Annual Forum, 2010.

[11]Yomchinda, T., Grande, N., Langelaan, J. W., and Horn, J. F., "Development and Testing of an Autonomous Autorotation System," Unmanned Rotorcraft and Network Centric Operations Specialists' Meeting, Junuary 22-24 2013.

[12]"MIL-STD-1797A: Flying Qualities of Piloted Aircraft," Technical report, Department of Defense, Washington DC, December 1997.

[13]Lee, A. Y., Jr., A. E. B., and Hindson, W. S., "Optimal Landing of a Helicopter in Autorotation," *Journal of Guidance, Control, and Dynamics*, Vol. 11, (1), January-February 1988, pp. 7–12.

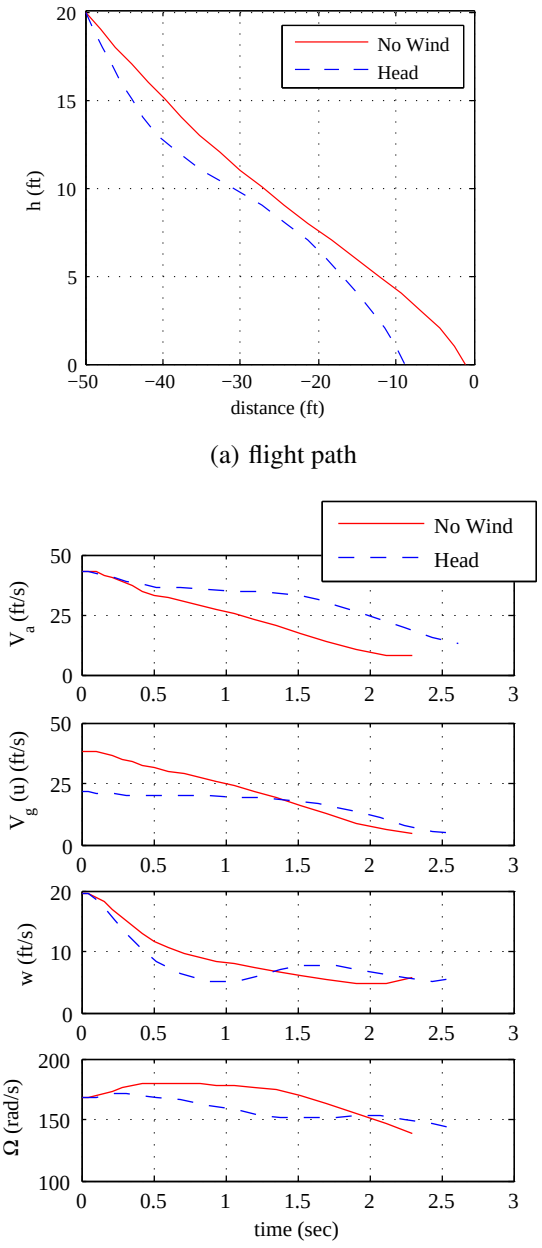

(a) flight path

(b) state history

Fig. 9. Flare trajectories and state history for the Hornet starting at the same initial conditions under light head wind and no wind conditions.

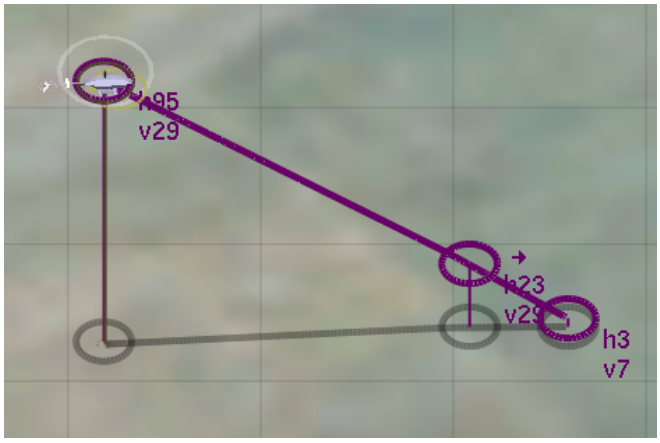

Fig. 10. Hornet simulation flare trajectory using three waypoints for entry, initiation, and touchdown.

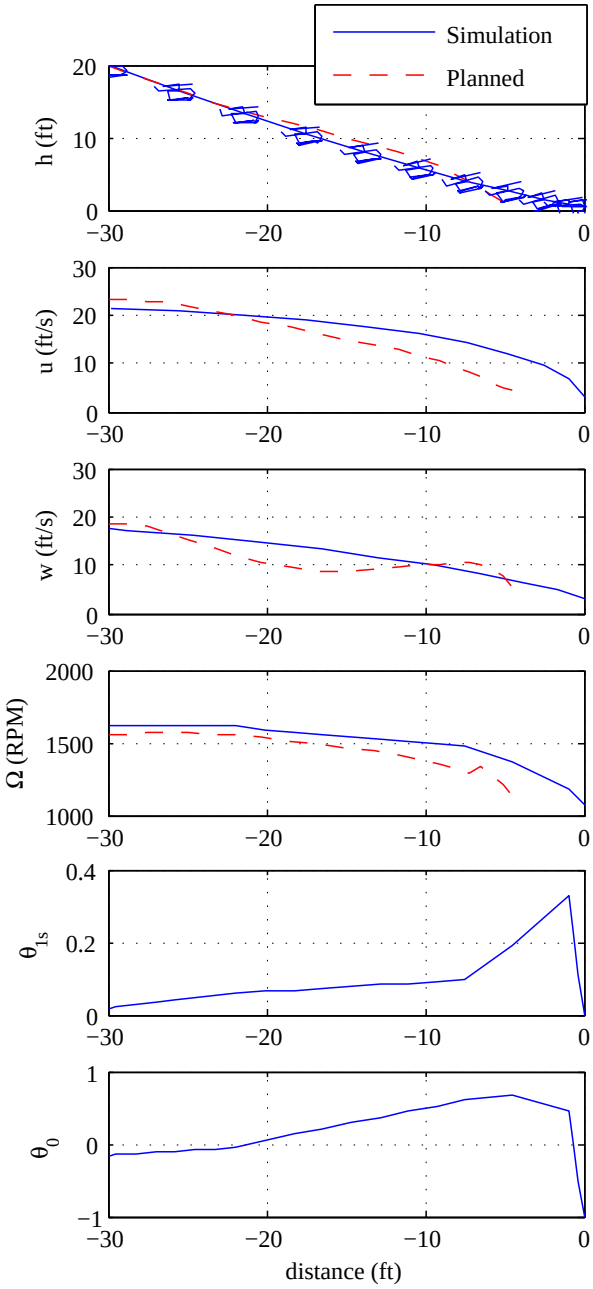

Fig. 11. Comparison of the planned Hornet flare maneuver with the simulated maneuver. The top image shows the planned trajectory and the simulated trajectory. The helicopter images show a snapshot of vehicle location and pitch orientation at 0.2 second intervals. θ_{1s} and θ_0 represent longitudinal cyclic pitch and collective pitch, respectively. (Note: the helicopter images are not drawn to scale)